Amazon fire regimes under climate change scenarios

Leonardo A. Saravia [1] [4], Ben Bond-Lamberty [2], Samir Suweis [3]

1. Instituto de Ciencias, Universidad Nacional de General Sarmiento, J.M. Gutierrez 1159 (1613), Los Polvorines, Buenos Aires, Argentina.

2. Pacific Northwest National Laboratory, Joint Global Change Research Institute, 5825 University Research Court #3500, College Park, MD 20740, USA

3. Laboratory of Interdisciplinary Physics, Department of Physics and Astronomy "G. Galilei", University of Padova, Padova, Italy

4. Corresponding author e-mail lsaravia@campus.ungs.edu.ar, ORCID https://orcid.org/0000-0002-7911-4398

Abstract

Fire is one of the most important disturbances of the earth-system, shaping the biodiversity of ecosystems and particularly forests. Anthropogenic drivers such as climatic change and other human activities could produce potentially abrupt changes in fire regimes, triggering more profound transformations like the transition from forests to savannah or grasslands ecosystems. Large biodiversity loss could be produced if these transitions occur. Climate change could enhance fire ignition and spread, potentially producing more extensive, intense, and frequent fires. In this work, we evaluate the possible changes in the Amazon region's fire regime. We parameterize a fire model using remote sensing data on fire extension and temperature, by considering climate projections for the 21st century. In the context of our model, there are two possible regime changes: the critical regime that implies high variability in fire extension and mega-fires, and an absorbing phase transition which would produce the extinction of the forest and transition to a different vegetation state. The fitted model and the projections suggest that the Amazon region is not close to any of these regime changes, but other factors not included in the model could be crucial for determining the probability of such critical transitions.

Introduction

Very few regions in the terrestrial biosphere are unaffected by fire. Fires caused directly or indirectly by human activities [1] have different characteristics from natural fires, including in spatial pattern, severity, burn frequency and seasonality, producing contrasting ecological consequences [2]. Recent years have seen an increase in fire intensity and extension in different regions [1,3], partially attributable to the fact we are experiencing a biosphere that is 1°C above historical records [4]; also, it is hypothesized that this intensification could reduce the spatial and temporal variation in fire regimes, called pyrodiversity [5], that in turn will generate substantial reductions in biodiversity and ecosystem processes such as carbon storage [6,7]. Probably the most affected regions will be the ones in which fire has been historically rare or absent. In regions such as tropical forests [8], extreme fires could trigger extensive biodiversity loss as well as major ecosystems changes as transitions from forest to savannah or shrublands [9,10].

Fires in the Amazon region were historically rare, due to the ability of old-growth forest to maintain enough moisture to prevent fire spread, even after prolonged drought periods [11]. Human activities such as deforestation and land-use change over the past 40 years have produced the conditions for fire to become much more frequent and widespread across the basin [12,13]. Droughts are predicted to increase due to climatic change, and these events have the potential to interact with human activities such as secondary vegetation slash-and-burn and cyclical fire-based pasture cleaning [13]. Even if deforestation rates have been substan-

tially reduced until 2018 [14], the previous activities provide sufficient ignition sources for fire to expand into adjacent forests [13]. This process could increase the importance of fires unrelated to deforestation [15].

Different models of fire for the Amazon have been developed to predict regime changes under climate change scenarios. These models can be process-based [16] or statistical [17], and generally consider land-use change and other human activities, as well as local weather conditions, but they usually neglect the spatial dynamics of fire spread. Statistical fire models take into account mainly environmental factors [18], while others simulate more detailed processes [19], and a few treat spatial dynamical phenomena [20]. Such spatial dynamics are important because they can provide insights into how local interactions give rise to emergent fire patterns [21], and potentially change the stability characteristics of the entire dynamical system [22].

Simple models of fire have been used as an example of self-organized criticality (SOC), where systems can self-organize into a state characterized by power-laws in different model outputs. For example, the forest fire model of Drossel & Schwabl [23] (DSM) was proposed to show SOC in relation to the size distribution of disturbance events [24]. Power-laws imply scale invariance, meaning that there is no characteristic scale in the model. Later it was shown that DSM does not exhibit true scale invariance [25] and that the system needs to be somewhat tuned to observe criticality [26]. These facts diminished its theoretical attractiveness, but the model could be still of high practical relevance. Some modifications of the Drossell & Schwabl (DSM) model have been used to predict fire responses to climate change [27], and other DSM variants can reproduce features observed in empirical studies [28] such as the power-law distribution of the fire sizes, the size and shape of unburned areas and the relationship between annual burned area and diversity of ecological stages [29]. An analysis of different models showed that the key for reproducing all these patterns was changing the scale of grid cells to represent several hectares, and the 'memory effect': flammability increases with the time since the last fire at a given site [29,30]. But the exponent of the fire size distribution observed in different ecoregions still cannot be reproduced by these models.

These simple models could have critical behaviour characterized by power-law distribution in fire sizes and other model outputs. Such dynamics can be explained in terms of percolation theory [31] where there is a transition between two states: one where propagation of fires occurs, and another where it is very limited. The narrow region where the transition occurs is the critical point, characterized by an order parameter (fire size) that depends on some external control parameter (e.g. ignition probability) [32].

An example of this transition could be the case of the recent Australia 2019-2020 mega-fires [33]. Historically, indigenous fire stewardship in Australian landscapes maintained flammable forest in a disconnected state by producing frequent small scale fires [34]. This regime was disrupted by fire suppression related to European

colonization land-use change [35] and climate [36], pushing the system towards a critical regime [37]. These kinds of extreme events are very difficult to predict by Earth system models that do not fully incorporate the dynamic of fuel accumulation and vegetation dynamics [38].

The objective of this work is to predict the fire regimes of the Amazon region based on climate change scenarios using a simple spatial stochastic fire model. By doing this we are assuming that the emergent dynamics can be described by a process of slow accumulation of fuel and rapid discharge produced by the fires. We first analyse the fire dynamics of the last 20 years in the region with the MODIS burnt area product to check our main assumption and derive an ignition probability. Then we predict the ignition probability up to the year 2060 based on different greenhouse gas Representative Concentration Pathways. Finally, using the model forced with the ignition probability, we predict and analyse the possible changes in the fire regimes for the Amazon.

Methods

Our region of study is the Amazon Basin (Figure S1). This includes Brasil, which represent 60% of the area, as well as eight other countries (Bolivia, Colombia, Ecuador, Guyana, Peru, Suriname, Venezuela, and French Guiana). We choose this region because a significant amount of fires extend to tropical moist forest outside Brasil [39], and the whole area is thought to be a crucial tipping element of the Earth-system [40,41].

Fire data and parameters

We estimated the monthly burned areas from 2001 to the end of 2021 using the NASA Moderate-Resolution Imaging Spectroradiometer (MODIS) burnt area Collection 6 product MCD64A1 [42], which has a 460 m pixel resolution. To download the data we used Google Earth Engine restricted to the region of interest. Each image represents the burned pixels as 1 and the non-burned as 0. We then calculated the burned clusters using 4 nearest neighbours (Von Neumann neighbourhood) and the Hoshen–Kopelman algorithm [43]. Each cluster contains contiguous pixels burned within a month and this represents a fire event S, allowing us to calculate the number and sizes of fire clusters by month. We estimated the probability of ignition f as $f(t) = \frac{|S_t|}{T}$, where $|\ |$ denotes the number of clusters, S_t that start in the month t (if a fire started in the previous month we avoided it to remove possible double counting), and T is total number of pixels in the region, to allow comparisons with the fire model.

We also estimated the distribution of fire sizes using an annual period to have enough fire clusters to discriminate between different distributions. We aggregated the monthly images using a simple superposition; the annual image has a 1 if it has one or more fires during the year, and 0 if it has none. This assumes that

most of the sites only burns once a year, we verified this using the MODIS data that on average only a 0.06% burn more than once annually. After that, we ran again the Hoshen–Kopelman algorithm and obtained the annual fire clusters and fitted the following distributions to the fire sizes: power-law, power-law with exponential cut-off, log-normal, and exponential. We used maximum likelihood to decide which distribution fit the data best using the Akaike Information Criteria (AIC) [44]. Additionally, we computed a likelihood ratio test, Voung's test [45], for non-nested models. We only considered it a true power-law when the value of the AIC was at a minimum and the comparison with the exponential distribution using the Vuong's test was significant with p<0.05; if p>=0.05 we assumed that the two distributions cannot be differentiated.

Modelling the probability of ignition

We calculated the monthly ignition probability f and related it to monthly precipitation (ppt), maximum temperature (T_{max}) and a seasonal term (m). These variables have generally been included in global and regional fire activity models [17,18,46,47]. More variables were used in these models, but we are constrained by the variables available in the Climate Projections (see below). We obtained environmental data from the TerraClimate dataset [48], doing an average over the region of study, aiming to represent the influence of regional climate over f. We transformed f to logarithms, because it had a highly skewed distribution, and evaluated an increasingly complex series of generalized additive models (GAMs), assuming a Gaussian distribution family. We used thin plate regression splines [49] as smoothing terms, and for interactions between environmental variables we used tensor products, using restricted maximum likelihood (REML) to fit to the data [49]. All these procedures were available in the R package **mgcv** [50] and all source code is available at the repository https://github.com/lsaravia/AmazonFireTippingPoints.

We selected the best model using AIC [50]. To evaluate the predictive power of the models, we broke the data set into a training set representing 85% of the data (with Date < 2018) and testing set (with Date >= 2018). The testing set was always 3 years long and we repeated the procedure starting at different dates. We then calculated the mean absolute percentage error (MAPE) for the three best models selected with AIC (Table S2). The formula of the MAPE is as follows:

$$\text{MAPE} = \frac{100}{N_{tot}} \sum_{i=1}^{N_{tot}} \frac{|n_i^{obs} - n_i^{pred}|}{n_i^{obs}}$$

We used the previously-described GAM model to obtain predictions of the ignition probability up to 2060. Driving data were obtained from the NASA Earth Exchange Global Daily Downscaled Climate Projections NEX-GDPP (https://www.nccs.nasa.gov/services/data-collections/land-based-products/nex-gddp)[51], which were estimated with General Circulation Models (GCM) runs conducted under the Coupled Model Intercomparison Project Phase 5 [52]. We averaged over the 21 CMIP5 models and over the study region

to obtain the monthly values of the needed variables: precipitation and maximum temperature. Then we estimated the probability of ignition up to 2060 using the fitted GAM across two of the four Representative Concentration Pathways (RCPs), RCP4.5 and RCP8.5 [53]. Such RCPs are greenhouse gas concentration trajectories adopted by the IPCC and used for climate modelling and research [54].

Fire Model

Conceptually the model represents two processes: forest burning and forest recovery. We assume that the forest layer represents the flammable forest (rather than forest cover), and that when a site is burned it does not mean that all the vegetation is dead, but that all the fuel is consumed.

The model uses a 2-dimensional lattice to represent the spatial region. Each site in the lattice can be in one of three different states: an empty or burned site, a flammable forest (called forest for short), or a burning forest. The lattice is updated in parallel, according to the following steps:

1. We pick at random a burning site, and it becomes an empty site in the following step (the model's timestep is one day)
2. We pick at random a forest site and it becomes a burning forest if one or more of its four nearest neighbour sites are burning
3. We pick at random another forest site and it sends (with probability p) a propagule to an empty site at a distance drawn from a power-law dispersal kernel with exponent de.
4. A random site can catch fire spontaneously with probability $f(\mathrm{t})$, i.e., this probability changes by month, reflecting the fire season.

We assumed absorbing boundary conditions and a lattice size of 450x450 sites, but also ran simulations with other sizes, resulting in equivalent results. Rule 3 means that a burned or empty site can become forest more quickly when it is near a forest site, but also that some sites can become forest even when far from established forest sites–depending on the kernel exponent, it could be any site in the lattice [55]. The choice of a power-law dispersal is justified because forests dispersion generally exhibits fat-tailed kernels [56,57].

This model is very similar to the Drossel-Schwabl forest fire model [23]: it exhibits critical behaviour when $\theta = p/f$ tends to ∞, and thus must satisfy the condition that $f << p$, as is generally observed in natural systems. The model involves the separation between three time scales: the fast burning of forest clusters, the slow recovery of forest, and the even slower rate of fire ignitions. Then in the critical regime there is a slow accumulation of forest that forms connected clusters, and eventually as the ignition probability is very low

these clusters connect the whole lattice— here is the link with percolation theory [31]— and a single ignition event can produce big fires. After this, the density of the forest becomes very low and the accumulation cycle begins again. This regime is characterized by wide fluctuations in the size of fires and the density of trees, with both following approximately power-law size distributions. If the ignition probability f is too high fires are frequent, forest sites become disconnected and small fires, with a characteristic size, dominate the system.

One of the features not present in the original forest fire model is that forests can have long-distance dispersal, modifying the distribution of forest clusters, the distribution of fire sizes, and the dynamics of the model. When forest dispersal is limited mainly to nearest neighbours, forest recovery produces clusters that tend to coalesce and form uniform clusters with few or no isolated forest sites. When the forest burns, these isolated forest sites are the points from where the forest recovers (assuming no external colonization); when these are not present there is an increased probability that the forest becomes extinct. When dispersal is long-distance there is an important number of isolated forest sites, thus decreasing the probability of forest extinction. All these processes are particularly important when θ is low and fires are smaller but more frequent. In dynamical terms there is a critical extinction value θ_{ext}, when $\theta < \theta_{ext}$ the forest become extinct, but the critical value depends on the dispersal distance governed by de.

The second feature not present in the original forest fire model is seasonality. In natural systems, there is a period of the year when environmental conditions produce an increase in the fire ignition probability, and during the rest of the year there is a much lower probability of fires. This forces a periodic accumulation of forest and a short period of intense fires which is called the fire season. Thus, the model has a short period of low θ_{min} and a longer period of high θ_{max}. If both the minimum and maximum θ are in the critical region, the model behaviour, in the long run, will be like the critical regime with maximum fire sizes in the fire season. When θ_{max} is in the critical and θ_{min} outside the critical zone, the model's dynamics regime could have more extreme fires (i.e. be more similar to the critical regime) than an equivalent non-seasonal model. If both θ are outside the critical region the dynamics could be close to the critical extinction zone, but in this case, seasonal differences in fire sizes will be less pronounced.

Increasing the length of the fire season as predicted in climate change scenarios [58] will produce the model to spend more time at a lower θ decreasing the connectivity of the forest and the size of fires. Moreover, this could increase the possibility of critical extinction if $\theta_{max} - \theta_{min}$ are below θ_{ext}. In this work we are assuming that the forest is flammable forest; the extinction of this state could mean that environmental conditions become wetter and the forest does not burn anymore. If environmental conditions become dryer the extinction of forest probably means a transition to another type of vegetation and then the conditions

to apply this model will no longer hold.

We made a set of exploratory simulations, with a range of parameters compatible with what we found for the Amazon region, to characterize the previously described regimes (Table S3). Using a lattice size of 450x450 sites, we ran the simulations for 60 years with an initial forest density of 0.3 (we found that different initial conditions gave similar results), and used the final 40 years to estimate the total annual fire size, the maximum cluster fire size, the distribution of fire sizes, and the total number of fires. To determine the cluster fire sizes and distributions we used the same methods described previously for the MODIS fire data. We ran a factorial combination of dispersal exponent de and θ and 10 repetitions of each parameter set. First, we ran the experiment with θ fixed, keeping the ignition probability f constant, and then repeated the experiment with seasonality: we simulated a fire season of 3 months each year multiplying f by 10. A dispersal exponent $de >> 1$ (e.g. $de = 102$) is equivalent to a dispersal to the nearest neighbours, while $de = 2.0155$ corresponds to a mean dispersal distance of 66 sites (Table S3), i.e. long range dispersal.

Fire Model Fitting

As we already estimated the f parameter from the 20 years of MODIS data, we only needed to estimate the dispersal exponent de and the probability p of forest growth. This parameter p is expressed as $r = 1/p$, representing the average number of days for forest to recover. For this estimation we duplicated the extension of the estimated f as if it started in 1980; we allowed 20 years for transient effects to dissipate in the model, and then used the last 20 years to compare with monthly fire data. This choice was justified because most human activities in the Amazon started in this decade during the conversion of large areas of forest to agriculture [59].

To explore the parameter space we used Latin-hypercube sampling [60] with parameter ranges $4 - 2.0101$ for de and $90 - 7300$ days for r. We used 500 samples and 10 repeated simulations of the model for each sample, totalling 5000 simulations, as the model has a long transient period. We performed simulations with different starting forest density of 0.3 and 0.6 and selected the 10 best parameter sets using the ones with the minimum MAPE comparing the relative monthly fire size i.e the absolute size divided by the total number of sites (the number of MODIS pixels for the Amazon basin or the number of lattice sites for simulations) . We also calculated the correlation of the monthly observed data with model predictions. We observed low correlations due that the peaks in the model are delayed by 2-3 months; the same happens in more realistic process based models [19], and as we were not interested in predicting the exact seasonal fire patterns, we re-fitted the parameters with MAPE, but using the monthly maximum fire size of the year. The second step of our fitting procedure was to take the 10 best fitted parameter sets and calculate the power-law fire

distribution, for doing this we ran 100 simulations for each of the parameters sets and then calculated the fire cluster distributions using the same methods explained previously.

Finally, we ran the model with the best fitted parameters, the ignition probability estimated from the MODIS data, and the ignition probability estimated with the GAM model for the period 2000-2020, to check if the data fit with the range of predictions. We performed the fitting using a lattice size of 450x450 sites, and as we used relative values (e.g. absolute fire size divided by the total number of sites) the model does not represent a defined scale.

Model Predictions

We used the best fitted parameter set and the predictions of the parameter f under RCP4.5 and RCP8.5 to make simulations up to 2060. We started simulations in the year 1980 as in the fitting procedure, but instead of using f derived directly from data we used the f obtained from the GAM model, allowing us to compare actual and predicted fires using the same method to obtain f. For these simulations we sampled each f for each month, assuming that $log(f)$ follows a normal distribution with the average and standard deviation given by the values obtained in the GAM model.

Results

The monthly fires follow a strong seasonal pattern with a maximum between September and October (Figure S2). We characterize the annual fire regime using the total fire size (total burned area) and the maximum fire cluster (the biggest fire event S_{max}). We note that the years with highest S_{max} are also years with high total fire size (Figure 1). The years 2007 and 2010 had the two highest S_{max} and they also have a power-law distribution (Table S1, Figures S3-S5). Power-law distributions are defined as $cS^{-\alpha}$ where c is constant, α the exponent and have an extra parameters: $S = x_{min}$, which is the minimum value for which the power-law holds. The constant c is given by the normalization requirement [61]. Only 6 of 20 years exhibit fire sizes following a power law distribution (Table S1), and some of such distributions have a range $[S_{max} - x_{min}]$ with the highest values compared to the years without power-laws , but there are also years with power-law and small range. These two extremes represent a pattern that we also observe in the fire model.

We fitted GAM models for the ignition probability f with single variables, and combinations of two interacting variables, the best model with lower AIC and lower MAPE was the interaction $T_{max} * m$ (Table S2). For the GAM fitted to the complete dataset we observe that the model does not capture the most extreme years of f (Figure S7), but the model fitted for the first years (< 2018) predicted the rest of the data well (Figure S8).

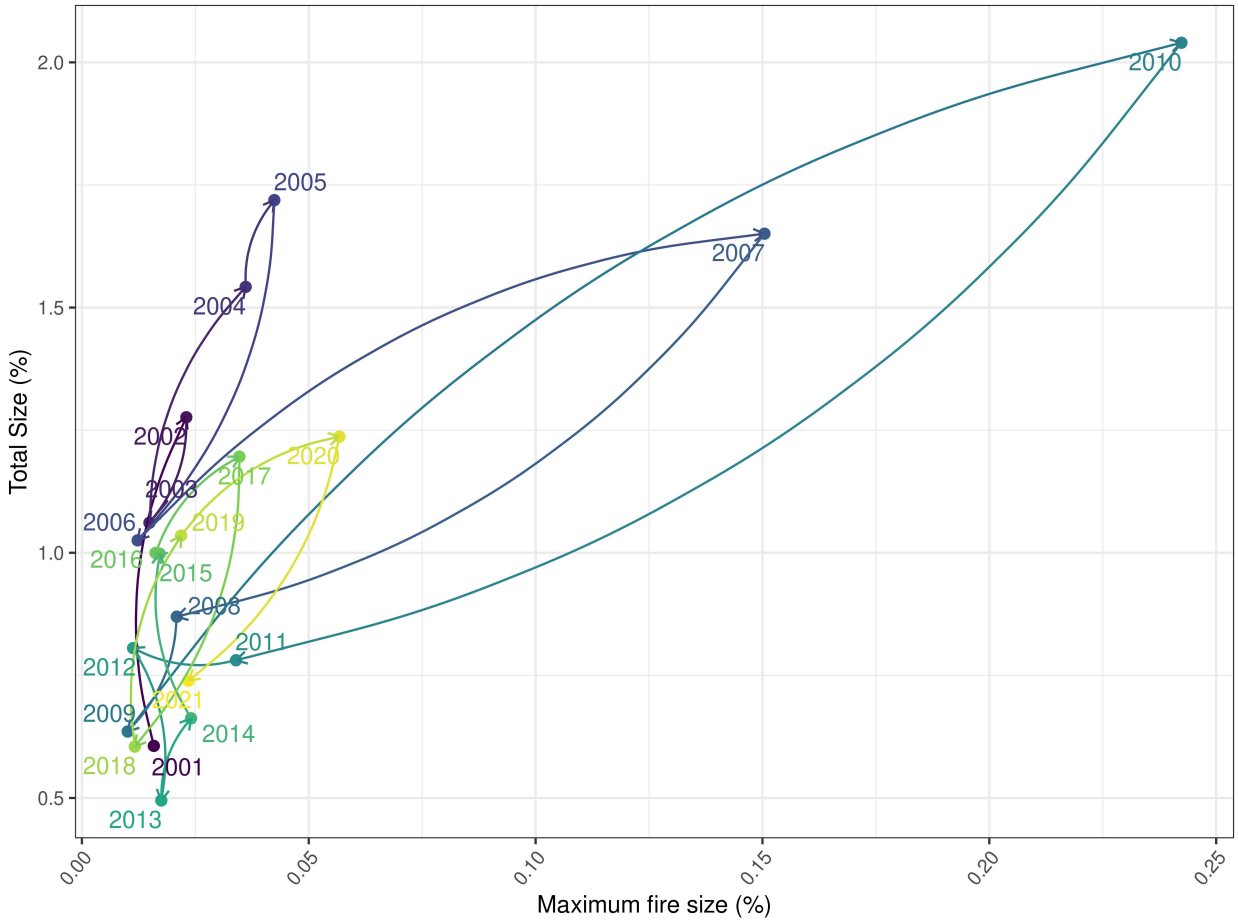

Figure 1: Annual total fire size vs maximum fire size relative to Amazon basin, estimated with MODIS burned area product. These observed data exhibit cycles of loading and discharge, years with high fire extension and big fire events—the upper right region of the figure—which are followed by years of low fire extension and no extreme events in the lower left region. A typical trajectory could be the years 2009, 2010 and 2011 where this cycle can be clearly observed.

With the best-fitted GAM and the T_{max} from the NASA Earth Exchange Global Daily Downscaled Climate Projections, we predicted the monthly f starting from 2020 for two greenhouse gas emissions scenarios: RCP4.5 and RCP8.5, in these cases, most data fall inside the standard error of the model (Figures S9 & S10)

Fire model exploration

We ran the model for a range of the $\theta = p/f$ parameter, anticipating that larger values would produce critical behaviour, consisting of large variability of fires between years and extremely large cluster fire sizes that follow a power-law distribution. As expected, we obtained a larger proportion of power-law distributions for the biggest size of θ (Table S4 & S5), and particularly high variability and extremely big fires (Figure 2). For simulations with seasonality, we observed the expected decrease on the number of years where fire cluster size follow power law distribution, also less variability and fewer extreme fires, because in these cases θ decreases for the fire season. Seasonality also had the unexpected effect of increasing the frequency of power-law distribution for $\theta = 25$ with a bigger exponent than the ones for large θ (Table S5); this pattern was also observed in the MODIS data.

In the simulations with θ 25 and 250 and with shorter dispersal distances, the forest density tends to decrease and eventually, it reaches zero, marking the absorbing phase transition reported for this type of model [37], meaning that in these cases the parameter θ was below the critical point θ_{ext} (Figure S11). Increasing the dispersal distance produces higher forest density, while seasonality has the opposite effect. In the case of high dispersal and low θ and seasonality, we are again below θ_{ext}. Note that forest density is the so-called active component of the model and represents the flammable forest.

Fire Model Fitting

We used two methods to fit the model to data, one using the monthly fire extent and another using the monthly maximum of the year, as the model produced delayed fire peaks. The first method resulted in very low values for the monthly maxima, which is also reflected in very low correlation values (Table S6, Figures S14 & S15). The second fitting method resulted in monthly fire time series more similar to data (Figure S14), with lower MAPE and higher correlation. For this reason, we used the parameters fitted with this last method for predictions. With the ten best parameter sets we calculated the power-law fire distribution and selected one parameter set with a median exponent closer to the data (Table S7). All these best parameters result in an average θ between 110 and 90 which is an intermediate range, considering the parameter range we used for the model exploration.

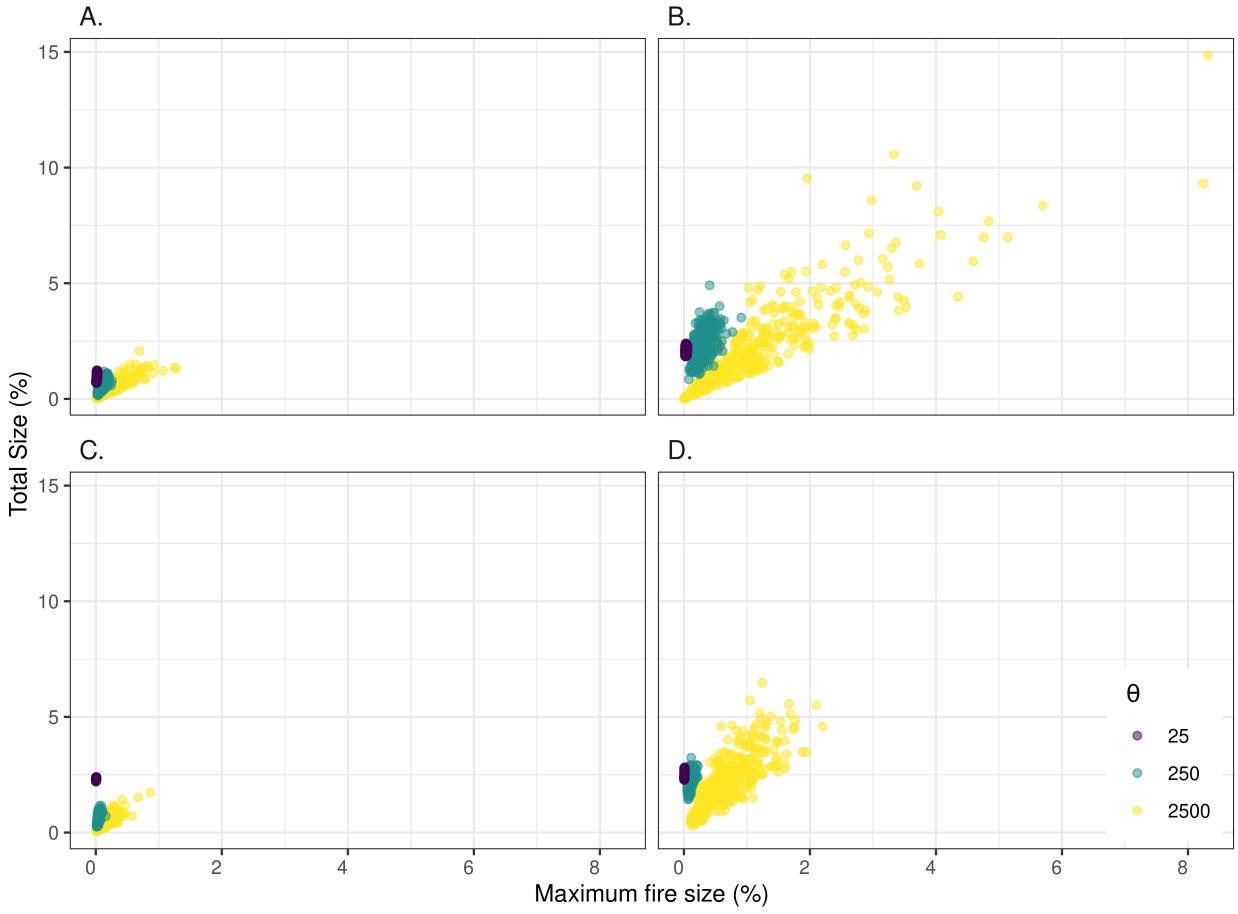

Figure 2: Total annual fire size vs. max fire cluster for the Fire model. **A** & **B** Are simulations with fixed θ, **A** with dispersal exponent $de = 102$, mean dispersal distance of 1 (equivalent to nearest neighbours) and **B** with $de = 2.0155$, mean dispersal distance of 66 sites. **C** & **D** Are simulations with a fire season of 90 days where θ is divided by 10 (the probability of ignition f is multiplied by 10), and the same de as previously.

When observing the predictions without temporal structure (Figure 3), the model simulated with the ignition probability f calculated from the data, and f estimated using the GAM model, gave results consistent with the observed data range. The predicted total fire size has a very good match with the data, while the predicted number of fires is slightly higher and S_{max} is slightly higher and the power-law exponent α of the fire size distribution is lower (Figure 3); these results are inter-related because when α is lower we expect larger fire events. (Figure 3). The modelled temporal series based on the f from data, closely follows the data for total fire size, overestimate the data with a systematic difference for number of fires, and is always bigger than the data for the max fire size S_{max} (Figure 4). The modelled temporal series that use the GAM estimated f showed an average response for total fires and do not followed data oscillations; the same average response is observed for the number of fires and S_{max}, overestimating the data in both cases.

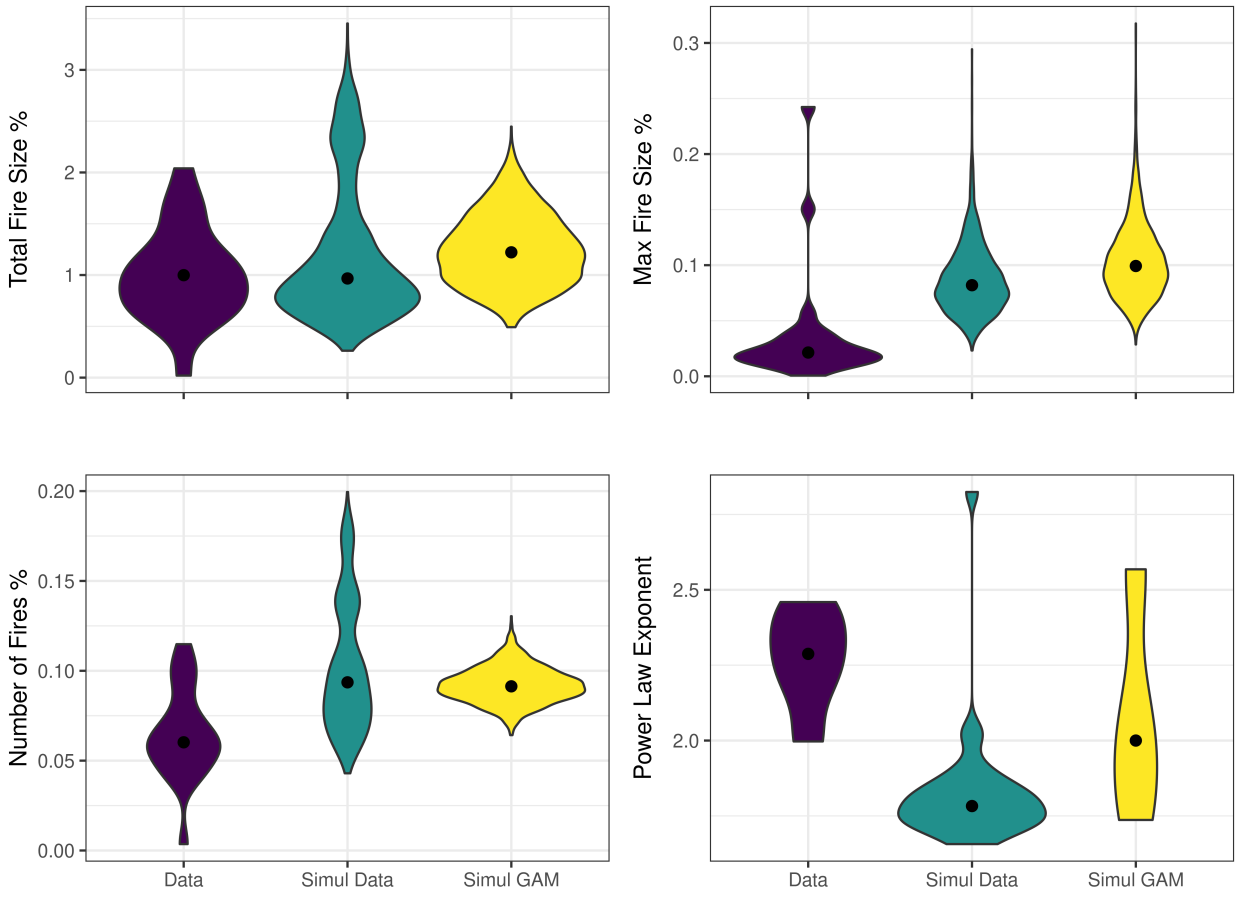

Figure 3: Predictions of the fire model compared with observed data for the years 2001-2020. We used best-fit parameters, the ignition probability from MODIS, and the ignition probability from the estimated GAM models (Simul GAM), and run 100 simulations of the model. All the outputs are relative to the total area; black points are the medians.

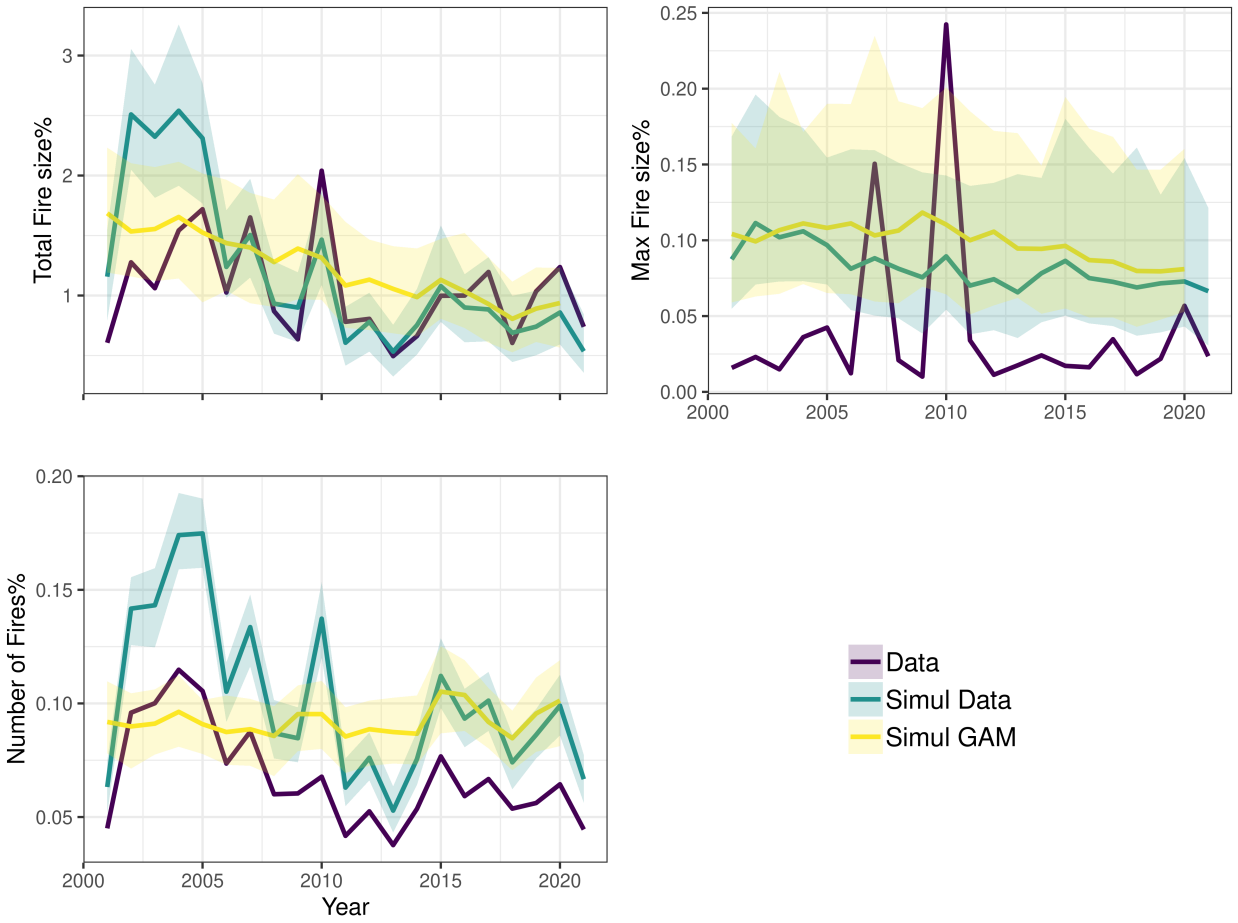

Figure 4: Time series of predictions of the fire model compared with observed ata for the years 2001-2020. We used best-fit parameters, the ignition probability from MODIS (Simul Data), and the ignition probability from the estimated GAM models (Simul GAM), and run 100 simulations of the model. The lines are the actual data or medians of simulations with 95% confidence interval bands. All the outputs are relative to the total area.

Fire model predictions

We observed that the θ for the best fitted parameter was in the lowest range if we consider the set of ten best fitted parameters (Table S7), so we decided to add simulations with other parameters from the set, but with the highest values of θ. Then we performed the simulations with the first row ($\theta \sim 90$) and the sixth row ($\theta \sim 110$) of the parameters in table S7. The simulations by decade gave results that are similar between the two RCPs (Figure 5). The simulations with $\theta \sim 110$ resulted in higher values of total fire and maximum fire, a difference that was more accentuated after the 2040s. The range of the predictions was, in all cases, lower than the range of the observed data.

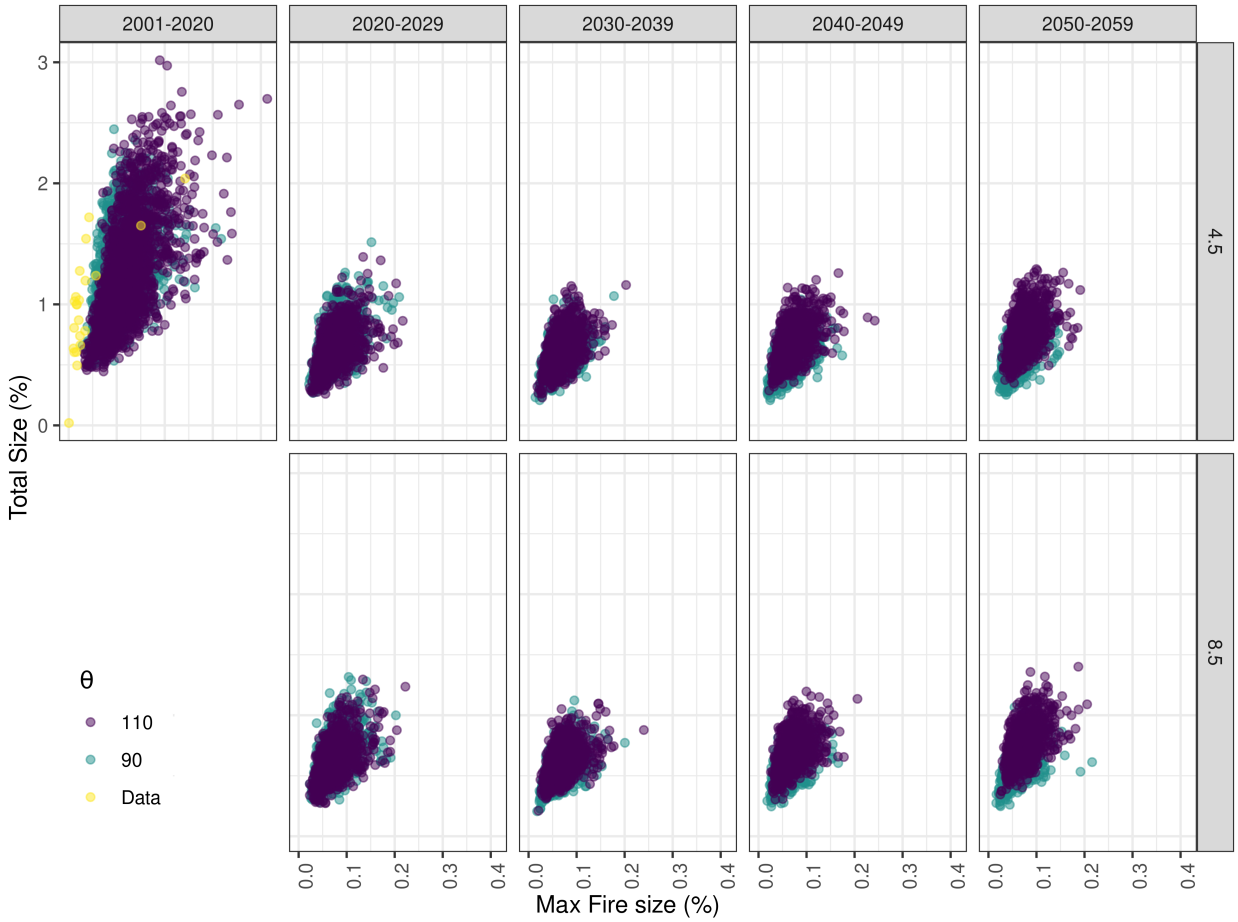

Figure 5: Total annual size of fires vs maximum fire size % relative to the area of the region. The data column was estimated using the MODIS burned area product. The predictions by decade were estimated with a fitted model using a monthly ignition probability calculated with data from General Circulation Models under two greenhouse gas emissions scenarios known as Representative Concentration Pathways (RCPs), RCP4.5 and RCP8.5. For the years 2001-2020 the ignition probability was estimated from actual data. We show two of the best fitted fire models with the minimum and maximum θ parameter.

Discussion

Based on spatial forest-fire dynamics, the model fitted to actual data and the predictions up to 2060 suggest that the Amazon fire dynamics are outside a critical regime and far from an absorbing phase transition. But the predictions based on an estimated ignition probability showed a qualitative fit to the data, and thus the level of confidence of these predictions are at most medium level. A critical regime would imply far more extreme fires and an absorbing phase transition could signal an imminent forest-savanna transition, without extreme fires but with more frequent fires. This model does not explicitly includes deforestation or slash and burn and other agricultural areas—these are implicitly represented in the flammable forest state—and thus the continuous increase of these land uses could change the dynamics of the model increasing the burned area. In its present form the model predictions represent the influence of climate change on Amazonian fire dynamics.

The actual and predicted fire regime seems to lie between these extremes, and all the predictions showed a decrease in maximum fire size and extension.

Similar models have been used to fit fire data and determine if the system is on a critical regime. For example, Zinck et al. [30] found that some regions of Canada have experienced a change in the fire regime from a non-critical to critical. They argued that the original Drossel-Schwabl model (DSM) did not give the correct values of the power-law exponent of fire distributions, thus they modify the model and represented fire propagation as a stochastic birth-death process. This means modelling fire as a contact process [62] that develops over the forest sites; the same concept was further explored concerning the recent Australian mega-fires [37]. Here we took a different approach: as in the DSM in our model fire spread is deterministic, and we added what we think are the minimal processes needed for more realism: seasonality and forest dispersal distance. We agree with Zinck et al. [30] that an extension of the original DSM was needed to represent fire process observed in ecosystems, but also that not all complexity can or should be added; it is necessary to keep the model tractable in order to e.g. perform parameter-space exploration. Similar models including a deforested state with different ignition f and recovery p probabilties should be built and a more rigorous comparison between these types of fire models would be needed to determine which mechanisms are most important to represent.

Our model is phenomenological, in the sense that it does not include all mechanisms present at local scales but tries to predict fire dynamics at broad scales. One of the advantages of this kind of model is that it can be applied to different systems. This is the case of the original DSM model which has been applied to brain activity and rainfalls [63]. In these two systems there are cycles of loading and discharge, a broad region where the fluctuations peak as the critical behaviour is established, and not a critical point with a very sharp

transition as the theory of second order phase transitions suggest [31]. The temporal dependence of the parameters imposed by the fire seasons, where during some months there is a higher ignition probability f, changes the control parameters with respect to the DMS model since, in fact, we do not observe a transition for a specific value of the θ parameter. Our results suggest that instead of having a specific fine-tuning to observe critical fire spread, a critical region similar to a Griffiths phase [64] may be present in our model. However, we lack a rigorous result in this regard.

We observed the expected effect of the drought in 2010 on fires: the Amazon basin experienced the most extensive fires of the record, despite the deforestation rates being substantially lower than in the previous decade [13]. Other years of drought did not have the same effect, and the drought associated with the El Niño event in 2015-2016 produced a considerably lower number of fires than the 2010 drought. This difference could be explained by the non-linear loading and discharge cycles that characterize the dynamics of fire-forest systems: after the fires and drought the fuel build up during the wetter years so the effects of an extreme could be different. It has been observed that deforestation as a cause of fires is becoming secondary, with droughts becoming primary producers of fires in the Amazon [13]. The good fit of our model forced with the ignition probability estimated from actual data, mainly after 2005, supports that hypothesis. Our model incorporates the influence of drought using actual and predicted temperature to model the probability of ignition f. Besides, a longer fire season is thought to produce an increase in fires [59], and our model showed that in the ranges of temperature predicted until 2060 over the two greenhouse gas emissions scenarios there no evidence of a substantial increase in fire extension or maximum fire size. More frequent fires produce on average smaller fire events with a lower variability, and a low probability of mega-fires.

The forest state in the model represent the flammable forest, as undisturbed tropical forest in the Amazon is thought to be not flammable and with a very low probability of natural fires [17]. This is changing, however, due to the increased edges of undisturbed forest with human degraded forest and other land uses [13]. Fire is still produced by human activities [8] and starts from the transportation network and from the outside regions [59]. These human-induced fires can invade standing forest and if climate change makes forests hotter and drier it will become more capable of sustaining more extensive fires [59]. All these changes are not considered in our model, and they would imply a higher density of our flammable forest state that could be represented by a lower θ than the estimated one, and increase the likelihood of an absorbing phase transition in which the forest has lost its capacity to recover from frequent fires and droughts [59]

Different authors have suggested that a deforestation of 20%-40% of the Amazon will produce a rapid transition to non-forest ecosystems [65,66]. Currently, approximately 20% of the forest since the 1960s has been lost, and environmental signals suggest that the system as a whole is oscillating [65]; dynamical analysis

predicts that it is close to a transition [67]. Our model predicts that the fire regime will not have an important variation due only to climatic change. Our main conclusion is that if deforestation and degradation of the Amazon forest stop, the Amazon will probably be resilient to predicted climatic change and the collapse of the Amazonian tropical forest towards a savannah will not be observed.

Acknowledgements

We are grateful to the National University of General Sarmiento for financial support (Project 30/1139).

Authors' contributions

LAS, BBL, and SS conceived the ideas and designed methodology; LAS collected the data; LAS wrote the code; LAS, BBL and SS analysed the data; LAS led the writing of the manuscript. All authors contributed critically to the drafts and gave final approval for publication.

Data Availability Statement

The source code and data is available at zenodo https://doi.org/10.5281/zenodo.5703638 and Github https://github.com/lsaravia/AmazonFireTippingPoints. Remote sensing MODIS data and climate data are available directly from NASA and Google Earth Engine.

References

1. Bowman DMJS, Kolden CA, Abatzoglou JT, Johnston FH, van der Werf GR, Flannigan M. 2020 Vegetation fires in the Anthropocene. *Nature Reviews Earth & Environment*, 1–16. (doi:10.1038/s43017-020-0085-3)

2. Steel ZL, Collins BM, Sapsis DB, Stephens SL. 2021 Quantifying pyrodiversity and its drivers. *Proceedings of the Royal Society B: Biological Sciences* **288**, 20203202. (doi:10.1098/rspb.2020.3202)

3. Pivello VR *et al.* 2021 Understanding Brazil's catastrophic fires: Causes, consequences and policy needed to prevent future tragedies. *Perspectives in Ecology and Conservation* (doi:10.1016/j.pecon.2021.06.005)

4. Masson-Delmotte V *et al.*, editors. 2021 Summary for policymakers. In *Climate Change 2021: The Physical Science Basis. Contribution of Working Group I to the Sixth Assessment Report of the Intergovernmental Panel on Climate Change*, Cambridge University Press.

5. Kelly LT, Brotons L. 2017 Using fire to promote biodiversity. *Science* **355**, 1264–1265. (doi:10.1126/science.aam7672)

6. Dieleman CM *et al.* 2020 Wildfire combustion and carbon stocks in the southern Canadian boreal forest: Implications for a warming world. *Global Change Biology* **26**, 6062–6079. (doi:10.1111/gcb.15158)

7. Furlaud JM, Prior LD, Williamson GJ, Bowman DMJS. 2021 Bioclimatic drivers of fire severity across the Australian geographical range of giant Eucalyptus forests. *Journal of Ecology* **109**, 2514–2536. (doi:10.1111/1365-2745.13663)

8. Barlow J, Berenguer E, Carmenta R, França F. 2020 Clarifying Amazonia's burning crisis. *Global Change Biology* **26**, 319–321. (doi:10.1111/gcb.14872)

9. Hirota M, Holmgren M, Nes EHV, Scheffer M. 2011 Global Resilience of Tropical Forest and Savanna to Critical Transitions. *Science* **334**, 232–235. (doi:10.1126/science.1210657)

10. Fairman TA, Nitschke CR, Bennett LT, Fairman TA, Nitschke CR, Bennett LT. 2015 Too much, too soon? A review of the effects of increasing wildfire frequency on tree mortality and regeneration in temperate eucalypt forests. *International Journal of Wildland Fire* **25**, 831–848. (doi:10.1071/WF15010)

11. Uhl C, Kauffman JB. 1990 Deforestation, Fire Susceptibility, and Potential Tree Responses to Fire in the Eastern Amazon. *Ecology* **71**, 437–449. (doi:10.2307/1940299)

12. Alencar A, Asner GP, Knapp D, Zarin D. 2011 Temporal variability of forest fires in eastern Amazonia. *Ecological Applications* **21**, 2397–2412. (doi:10.1890/10-1168.1)

13. Aragão LEOC *et al.* 2018 21st Century drought-related fires counteract the decline of Amazon deforestation carbon emissions. *Nature Communications* **9**, 536. (doi:10.1038/s41467-017-02771-y)

14. Feng X *et al.* 2021 How deregulation, drought and increasing fire impact Amazonian biodiversity. *Nature* **597**, 516–521. (doi:10.1038/s41586-021-03876-7)

15. Aragão LEOC, Poulter B, Barlow JB, Anderson LO, Malhi Y, Saatchi S, Phillips OL, Gloor E. 2014 Environmental change and the carbon balance of Amazonian forests. *Biological Reviews* **89**, 913–931. (doi:10.1111/brv.12088)

16. Le Page Y, Morton D, Hartin C, Bond-Lamberty B, Pereira JMC, Hurtt G, Asrar G. 2017 Synergy between land use and climate change increases future fire risk in Amazon forests. *Earth System Dynamics* **8**, 1237–1246. (doi:10.5194/esd-8-1237-2017)

17. Fonseca MG, Alves LM, Aguiar APD, Arai E, Anderson LO, Rosan TM, Shimabukuro YE, de Aragão LEOeC. 2019 Effects of climate and land-use change scenarios on fire probability during the 21st century in the Brazilian Amazon. *Global Change Biology* **25**, 2931–2946. (doi:10.1111/gcb.14709)

18. Turco M, Jerez S, Doblas-Reyes FJ, AghaKouchak A, Llasat MC, Provenzale A. 2018 Skilful forecasting of global fire activity using seasonal climate predictions. *Nature Communications* **9**, 2718. (doi:10.1038/s41467-018-05250-0)

19. Thonicke K, Spessa A, Prentice IC, Harrison SP, Dong L, Carmona-Moreno C. 2010 The influence of vegetation, fire spread and fire behaviour on biomass burning and trace gas emissions: Results from a process-based model. *Biogeosciences* **7**, 1991–2011. (doi:10.5194/bg-7-1991-2010)

20. Schertzer E, Staver AC, Levin SA. 2014 Implications of the spatial dynamics of fire spread for the bistability of savanna and forest. *Journal of Mathematical Biology* **70**, 329–341. (doi:10.1007/s00285-014-0757-z)

21. Pueyo S, de Alencastro Graça PML, Barbosa RI, Cots R, Cardona E, Fearnside PM. 2010 Testing for criticality in ecosystem dynamics: The case of Amazonian rainforest and savanna fire. *Ecology Letters* **13**, 793–802. (doi:10.1111/j.1461-0248.2010.01497.x)

22. Levin SA, Durret R. 1996 From individuals to epidemics. *Philosophical Transactions of the Royal Society of London. Series B* **351**, 1615–1621. (doi:10.1098/rstb.1996.0145)

23. Drossel B, Schwabl F. 1992 Self-organized critical forest-fire model. *Physical Review Letters* **69**, 1629–1632. (doi:10.1103/PhysRevLett.69.1629)

24. Jensen HJ. 1998 *Self-Organized Criticality: Emergent Complex Behavior in Physical and Biological Systems*. Cambridge, U.K.: Cambridge University Press.

25. Grassberger P. 2002 Critical behaviour of the Drossel-Schwabl forest fire model. *New Journal of Physics* **4**, 17. (doi:10.1088/1367-2630/4/1/317)

26. Bonachela JA, Muñoz MA. 2009 Self-organization without conservation: True or just apparent scale-invariance? *Journal of Statistical Mechanics: Theory and Experiment* **2009**, P09009. (doi:10.1088/1742-5468/2009/09/P09009)

27. Pueyo S. 2007 Self-Organised Criticality and the Response of Wildland Fires to Climate Change. *Climatic Change* **82**, 131–161. (doi:10.1007/s10584-006-9134-2)

28. Ratz A. 1995 Long-Term Spatial Patterns Created by Fire: A Model Oriented Towards Boreal Forests. *International Journal of Wildland Fire* **5**, 25–34. (doi:10.1071/wf9950025)

29. Zinck RD, Grimm V. 2009 Unifying wildfire models from ecology and statistical physics. *The American naturalist* **174**, E170–85. (doi:10.1086/605959)

30. Zinck RD, Pascual M, Grimm V. 2011 Understanding Shifts in Wildfire Regimes as Emergent Threshold Phenomena. *The American Naturalist* **178**, E149–E161. (doi:10.1086/662675)

31. Stauffer D, Aharony A. 1994 *Introduction To Percolation Theory*. London: Tayor & Francis.

32. Solé RV, Bascompte J. 2006 *Self-organization in Complex Ecosystems*. New Jersey, USA.: Princeton University Press.

33. Nolan RH, Boer MM, Collins L, Dios VR de, Clarke H, Jenkins M, Kenny B, Bradstock RA. 2020 Causes and consequences of eastern Australia's 2019 season of mega-fires. *Global Change Biology* **26**, 1039–1041. (doi:10.1111/gcb.14987)

34. 2020 Biodiversity in flames. *Nature Ecology & Evolution* **4**, 171–171. (doi:10.1038/s41559-020-1119-4)

35. Hoffman KM *et al.* 2021 Conservation of Earth's biodiversity is embedded in Indigenous fire stewardship. *Proceedings of the National Academy of Sciences* **118**. (doi:10.1073/pnas.2105073118)

36. Adams MA, Shadmanroodposhti M, Neumann M. 2020 Causes and consequences of Eastern Australia's 2019 season of mega-fires: A broader perspective. *Global Change Biology* **26**, 3756–3758. (doi:10.1111/gcb.15125)

37. Nicoletti G, Saravia L, Momo F, Maritan A, Suweis S. 2021 The emergence of scale-free fires in Australia. *arXiv:2110.10014 [cond-mat]*

38. Sanderson BM, Fisher RA. 2020 A fiery wake-up call for climate science. *Nature Climate Change* **10**, 175–177. (doi:10.1038/s41558-020-0707-2)

39. Cardil A *et al.* 2020 Recent deforestation drove the spike in Amazonian fires. *Environmental Research Letters* **15**, 121003. (doi:10.1088/1748-9326/abcac7)

40. Lenton TM, Williams HTP. 2013 On the origin of planetary-scale tipping points. *Trends in Ecology & Evolution* **28**, 380–382. (doi:10.1016/j.tree.2013.06.001)

41. Staver AC, Archibald S, Levin SA. 2011 The Global Extent and Determinants of Savanna and Forest as Alternative Biome States. *Science* **334**, 230–232. (doi:10.1126/science.1210465)

42. Giglio L, Schroeder W, Justice CO. 2016 The collection 6 MODIS active fire detection algorithm and fire products. *Remote Sensing of Environment* **178**, 31–41. (doi:10.1016/j.rse.2016.02.054)

43. Hoshen J, Kopelman R. 1976 Percolation and cluster distribution. I. Cluster multiple labeling technique and critical concentration algorithm. *Physical Review B* **14**, 3438–3445. (doi:10.1103/PhysRevB.14.3438)

44. Clauset A, Shalizi C, Newman M. 2009 Power-Law Distributions in Empirical Data. *SIAM Review* **51**, 661–703. (doi:10.1137/070710111)

45. Vuong QH. 1989 Likelihood Ratio Tests for Model Selection and Non-Nested Hypotheses. *Econometrica* **57**, 307–333. (doi:10.2307/1912557)

46. Huang Y, Wu S, Kaplan JO. 2015 Sensitivity of global wildfire occurrences to various factors in the context of global change. *Atmospheric Environment* **121**, 86–92. (doi:10.1016/j.atmosenv.2015.06.002)

47. Wei F, Wang S, Fu B, Brandt M, Pan N, Wang C, Fensholt R. 2020 Nonlinear dynamics of fires in Africa over recent decades controlled by precipitation. *Global Change Biology* **26**, 4495–4505. (doi:10.1111/gcb.15190)

48. Abatzoglou JT, Dobrowski SZ, Parks SA, Hegewisch KC. 2018 TerraClimate, a high-resolution global dataset of monthly climate and climatic water balance from 1958. *Scientific Data* **5**, 170191. (doi:10.1038/sdata.2017.191)

49. Pedersen EJ, Miller DL, Simpson GL, Ross N. 2019 Hierarchical generalized additive models in ecology: An introduction with mgcv. *PeerJ* **7**, e6876. (doi:10.7717/peerj.6876)

50. Wood SN. 2017 *Generalized Additive Models: An Introduction with R, Second Edition*. CRC Press.

51. Thrasher B, Maurer EP, McKellar C, Duffy PB. 2012 Technical Note: Bias correcting climate model simulated daily temperature extremes with quantile mapping. *Hydrology and Earth System Sciences* **16**, 3309–3314. (doi:10.5194/hess-16-3309-2012)

52. Taylor KE, Stouffer RJ, Meehl GA. 2012 An Overview of CMIP5 and the Experiment Design. *Bulletin of the American Meteorological Society* **93**, 485–498. (doi:10.1175/BAMS-D-11-00094.1)

53. Meinshausen M *et al.* 2011 The RCP greenhouse gas concentrations and their extensions from 1765 to 2300. *Climatic Change* **109**, 213–241. (doi:10.1007/s10584-011-0156-z)

54. Moss RH *et al.* 2010 The next generation of scenarios for climate change research and assessment. *Nature* **463**, 747–756. (doi:10.1038/nature08823)

55. Marco DE, Montemurro MA, Cannas SA. 2011 Comparing short and long-distance dispersal: Modelling and field case studies. *Ecography* **34**, 671–682. (doi:10.1111/j.1600-0587.2010.06477.x)

56. Clark CJ, Poulsen JR, Bolker BM, Connor EF, Parker VT. 2005 Comparative seed shadows of bird-, monkey-, and wind-dispersed trees. *Ecology* **86**, 2684–2694.

57. Seri E, Maruvka, Shnerb NM. 2012 Neutral Dynamics and Cluster Statistics in a Tropical Forest. *The American Naturalist* **180**, E161–E173. (doi:10.1086/668125)

58. Pausas JG, Keeley JE. 2021 Wildfires and global change. *Frontiers in Ecology and the Environment* **19**, 387–395. (doi:10.1002/fee.2359)

59. Brando PM *et al.* 2019 Droughts, Wildfires, and Forest Carbon Cycling: A Pantropical Synthesis. *Annual Review of Earth and Planetary Sciences* **47**, 555–581. (doi:10.1146/annurev-earth-082517-010235)

60. Fang K-T, Li R, Sudjianto A. 2005 *Design and Modeling for Computer Experiments*. Boca Raton, FL.

61. Newman MEJ. 2005 Power laws, Pareto distributions and Zipf's law. *Contemporary Physics* **46**, 323–351. (doi:10.1080/00107510500052444)

62. Oborny B, Szabó G, Meszéna G. 2007 Survival of species in patchy landscapes: Percolation in space and time. In *Scaling Biodiversity*, pp. 409–440. Cambridge University Press.

63. Palmieri L, Jensen HJ. 2020 The Forest Fire Model: The Subtleties of Criticality and Scale Invariance. *Frontiers in Physics* **8**, 257. (doi:10.3389/fphy.2020.00257)

64. Moretti P, Muñoz MA. 2013 Griffiths phases and the stretching of criticality in brain networks. *Nature Communications* **4**, 2521. (doi:10.1038/ncomms3521)

65. Lovejoy TE, Nobre C. 2018 Amazon Tipping Point. *Science Advances* **4**, eaat2340. (doi:10.1126/sciadv.aat2340)

66. Nobre CA, Sampaio G, Borma LS, Castilla-Rubio JC, Silva JS, Cardoso M. 2016 Land-use and climate change risks in the Amazon and the need of a novel sustainable development paradigm. *Proceedings of the National Academy of Sciences* **113**, 10759–10768. (doi:10.1073/pnas.1605516113)

67. Saravia LA, Doyle S, Bond-Lamberty B. 2018 Power laws and critical fragmentation in global forests. *Scientific Reports* **8**, 17766. (doi:10.1038/s41598-018-36120-w)